

Separation of pyrrolidine from tetrahydrofuran by pillar[6]arene-based nonporous adaptive crystals

Jiajun Cao,^{a,†} Yitao Wu,^{a,†} Qi Li,^a Weijie Zhu,^a Zeju Wang,^a Yang Liu,^a Kecheng Jie,^a Huangtianzhi Zhu,^{a*} Feihe Huang^{a,b,c,*}

[a] J. Cao, Y. Wu, Q. Li, W. Zhu, Z. Wang, Y. Liu, Dr. H. Zhu, Prof. Dr. F. Huang

State Key Laboratory of Chemical Engineering, Stoddart Institute of Molecular Science, Department of Chemistry, Zhejiang University, Hangzhou 310027, P. R. China, Fax and Tel: +86-571-8795-3189, E-mail: htzzhu@zju.edu.cn, fhuang@zju.edu.cn

[b] Prof. Dr. F. Huang

ZJU-Hangzhou Global Scientific and Technological Innovation Center, Hangzhou 311215, China

[c] Prof. Dr. F. Huang

Green Catalysis Center and College of Chemistry, Zhengzhou University, Zhengzhou 450001, P. R. China

[†] These authors contributed equally

Electronic Supplementary Information (ESI, 22 pages)

1. <i>Materials</i>	S3
2. <i>Methods</i>	S3
3. <i>Crystallography Data</i>	S5
4. <i>Characterization of Activated Pillararene Crystals</i>	S7
5. <i>Vapor-Phase Adsorption Measurements</i>	S10
6. <i>Recyclability of EtP6β</i>	S21
7. <i>References</i>	S22

1. Materials

All reagents were commercially available and used as supplied without further purification. Solvents were either employed as purchased or dried according to procedures described in the literature. Pillar[*n*]arenes (**EtP5** and **EtP6**) were synthesized as described previously.^{S1} Activated crystalline **EtP5** and **EtP6** were referred to as **EtP5 α** and **EtP6 β** , respectively. **EtP5 α** and **EtP6 β** were prepared according to reported procedures.^{S2}

Table S1. Physical properties of pyrrolidine and THF

Substance	Melting point (°C)	Boiling point (°C)	Saturated Vapor Pressure at 298 K (kPa)
Pyrrolidine	-63.0	87.0	1.80
THF	-108	66.8	19.3

2. Methods

2.1. Powder X-Ray Diffraction

PXRD data were collected on a Rigaku Ultimate-IV X-Ray diffractometer operating at 40 kV/30 mA using the Cu K α line ($\lambda = 1.5418 \text{ \AA}$). Data were measured over the range of 5–45° in 5°/min steps over 8 min.

2.2. Thermogravimetric analysis

Thermogravimetric analysis (TGA) was carried out on a DSCQ1000 Thermal Gravimetric Analyzer with an automated vertical overhead thermobalance. The samples were heated in 10 °C/min steps over 8 min.

2.3. Single Crystal Growth

Single crystals of guest-loaded **EtP5** and **EtP6** were grown by volatilization: 5.00 mg of dry **EtP5** or **EtP6** powder were put in a small vial where 1.00 mL of guest was added and the vial was heated until all the powder was dissolved. The crystals were got by volatilization for 2-7 days.

2.4. Single Crystal X-ray Diffraction

Single crystal X-ray diffraction data were collected on a Bruker D8 VENTURE CMOS X-ray diffractometer with graphite monochromatic GaK α radiation ($\lambda = 0.71073 \text{ \AA}$).

2.6. Solution ^1H NMR Spectroscopy

^1H NMR spectra were recorded using a Bruker Avance DMX 400 spectrometer and a Bruker Avance DMX 600 spectrometer.

2.7. Gas Chromatography

Gas chromatographic (GC) analysis: GC measurements were carried out using an Agilent 7890B instrument configured with an FID detector and a DB-624 column ($30 \text{ m} \times 0.53 \text{ mm} \times 3.0 \text{ }\mu\text{m}$). Samples were analyzed using headspace injections and were performed by incubating the sample at $70 \text{ }^\circ\text{C}$ for 10 min followed by sampling 1.00 mL of the headspace. The total volume of the container was 10 mL; the mass of the solid in the container was about 10 mg; the total volume of the headspace was 1 mL. The following GC method was used: the oven was programmed from $50 \text{ }^\circ\text{C}$, and ramped in $10 \text{ }^\circ\text{C min}^{-1}$ increments to $150 \text{ }^\circ\text{C}$ with 15 min hold; the total run time was 25 min; the injection temperature was $250 \text{ }^\circ\text{C}$; the detector temperature was $280 \text{ }^\circ\text{C}$ with nitrogen, air, and make-up flow-rates of 35, 350, and 35 mL min^{-1} , respectively; helium (carrier gas) flow-rate was 3.0 mL min^{-1} . The samples were injected in the split mode (30:1).

3. Crystallographic Data

Table S2. Experimental single crystal X-ray data for the pyrrolidine@**EtP5** structure

	pyrrolidine@ EtP5
Crystallization Solvent	Pyrrolidine
Empirical formula	C ₆₁ H ₈₂ N _{1.5} O ₁₀
Formula weight	996.28
Temperature/K	170
Crystal system	triclinic
Space group	P-1
a/Å	14.9616(5)
b/Å	16.3732(6)
c/Å	24.4025(10)
α/°	109.598(3)
β/°	98.054(2)
γ/°	90.000(2)
Volume/Å ³	5568.9(4)
Z	4
ρ _{calc} /cm ³	1.188
μ/mm ⁻¹	0.408
F(000)	2154
Crystal size/mm ³	0.16 × 0.15 × 0.06
Radiation	GaKα (λ = 1.34139)
2θ range for data collection/°	5.764 to 110.29
Reflections collected	19009
Independent reflections	19009 [R _{int} = 0.0986, R _{sigma} = 0.1108]
Data/restraints/parameters	19009/30/1327
Goodness-of-fit on F ²	1.027
Final R indexes [I >= 2σ (I)]	R ₁ = 0.0986, wR ₂ = 0.2537
Final R indexes [all data]	R ₁ = 0.1502, wR ₂ = 0.3009
Largest diff. peak/hole / e Å ⁻³	1.26/-0.56
CCDC	2132123

Table S3. Experimental single crystal X-ray data for the pyrrolidine@**EtP6** and 2THF@**EtP6** structures

	pyrrolidine@ EtP6	2THF@ EtP6
Crystallization Solvent	pyrrolidine	THF
Empirical formula	C ₇₀ H ₈₉ NO ₁₂	C ₇₀ H ₉₂ O ₁₃
Formula weight	1136.42	1141.43
Temperature/K	193	213
Crystal system	orthorhombic	monoclinic
Space group	Fddd	P2/n
a/Å	12.5560(3)	12.5731(4)
b/Å	26.6378(7)	22.6648(7)
c/Å	45.7727(10)	14.4358(4)
α/°	90	90
β/°	90	113.995(2)
γ/°	90	90
Volume/Å ³	15309.3(6)	3758.2(2)
Z	8	2
ρ _{calc} /cm ³	0.986	1.009
μ/mm ⁻¹	0.342	0.349
F(000)	4896	1232
Crystal size/mm ³	0.06 × 0.06 × 0.05	0.07 × 0.07 × 0.05
Radiation	GaKα (λ = 1.34139)	GaKα (λ = 1.34139)
2θ range for data collection/°	8.444 to 109.904	7.656 to 109.988
Reflections collected	50740	38978
Independent reflections	3627 [R _{int} = 0.0588, R _{sigma} = 0.0262]	7131 [R _{int} = 0.0666, R _{sigma} = 0.0476]
Data/restraints/parameters	3627/70/225	7131/40/404
Goodness-of-fit on F ²	1.034	0.949
Final R indexes [I ≥ 2σ (I)]	R ₁ = 0.0929, wR ₂ = 0.2533	R ₁ = 0.0982, wR ₂ = 0.2222
Final R indexes [all data]	R ₁ = 0.1093, wR ₂ = 0.2659	R ₁ = 0.1261, wR ₂ = 0.2387
Largest diff. peak/hole / e Å ⁻³	0.67/-0.33	0.73/-0.33
CCDC	2132121	2132122

4. Characterization of Activated Pillararene Crystals

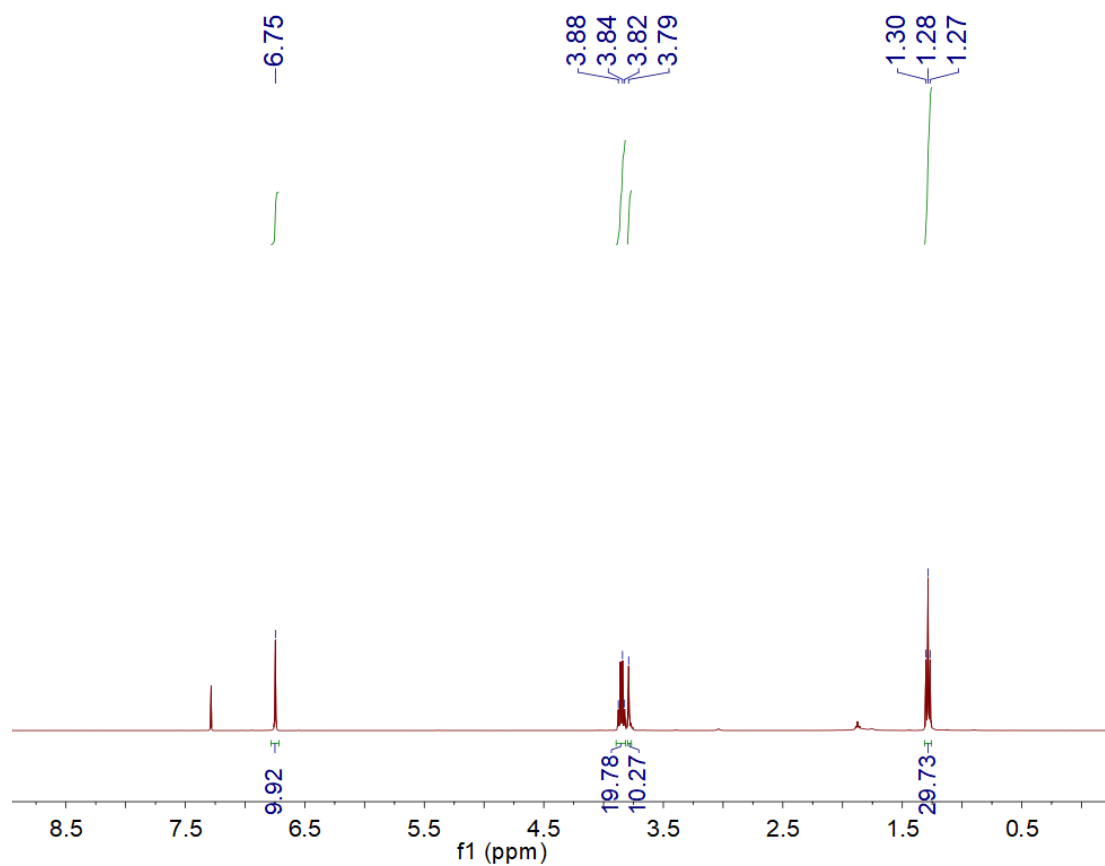


Fig. S1. ^1H NMR spectrum (400 MHz, CDCl_3 , 298 K) of **EtP5**.

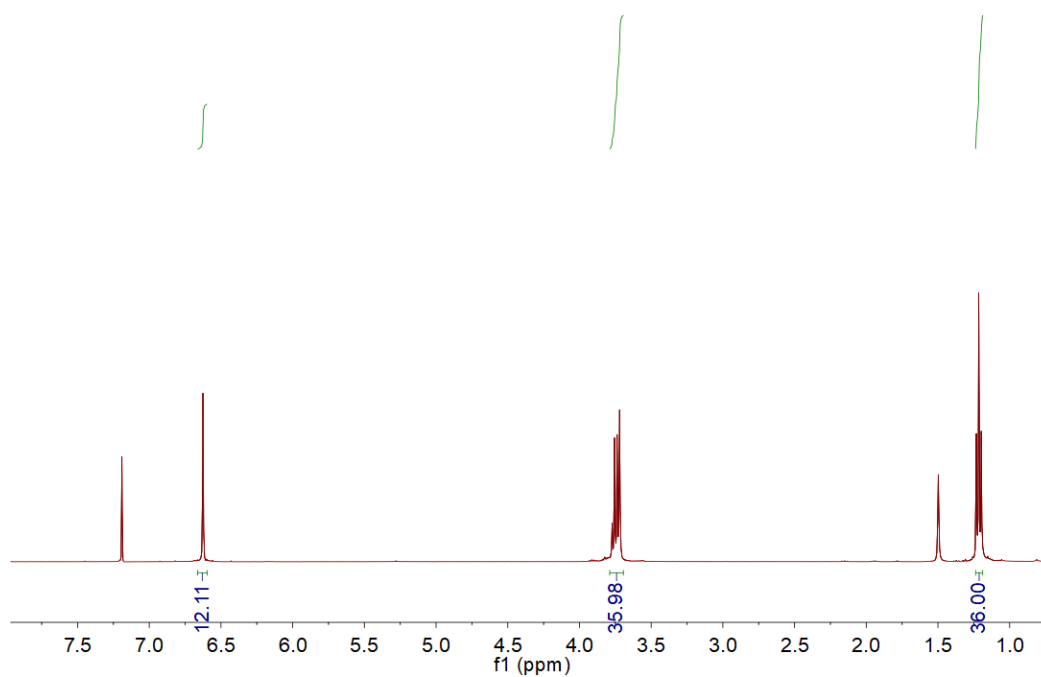


Fig. S2. ^1H NMR spectrum (400 MHz, CDCl_3 , 298 K) of **EtP6**.

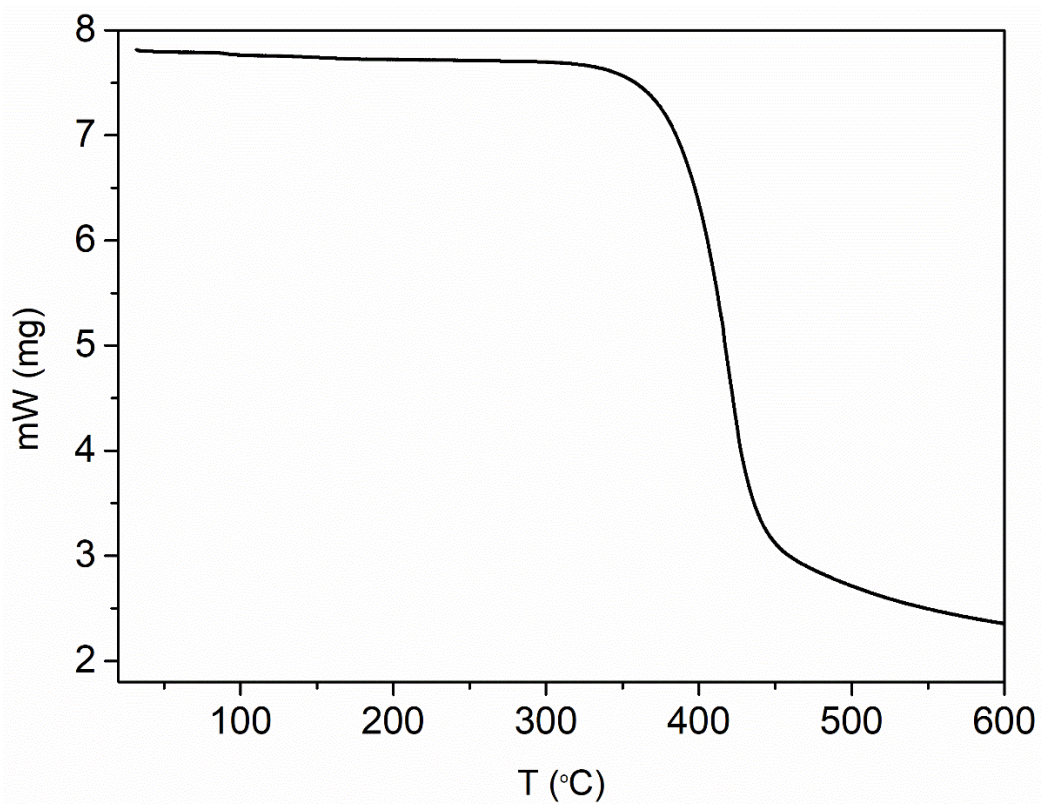


Fig. S3. TGA curve of desolvated **EtP5 α**

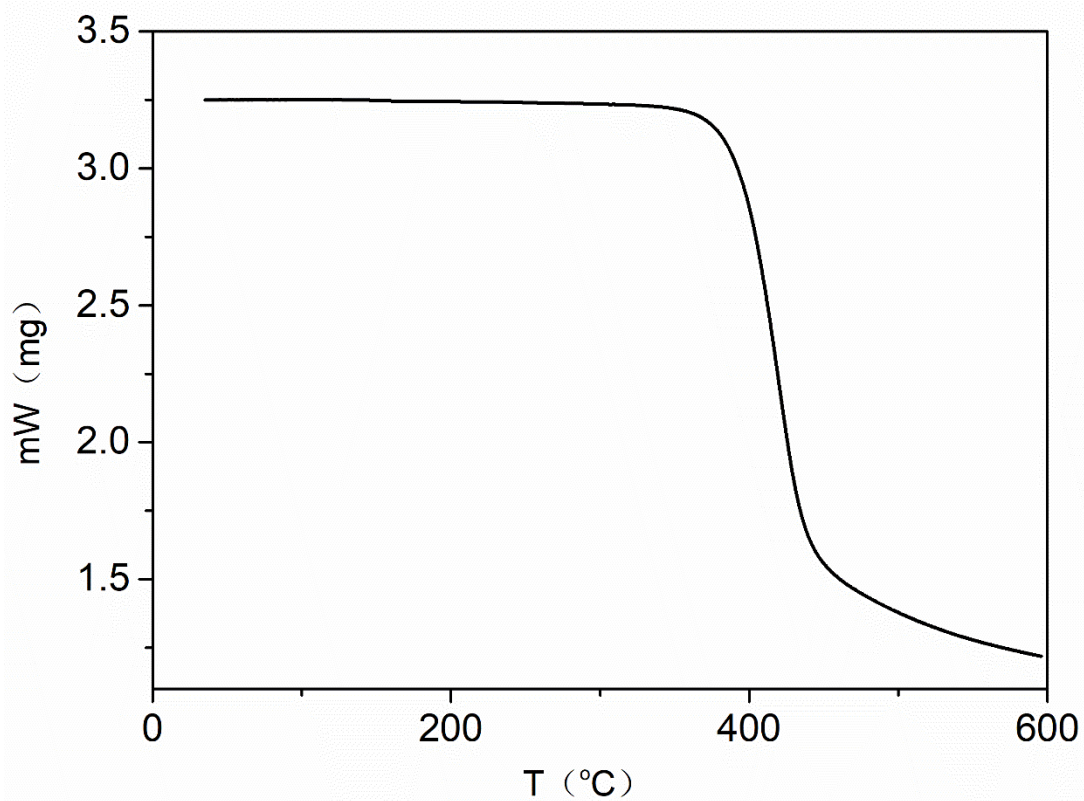


Fig. S4. TGA curve of desolvated **EtP6 β**

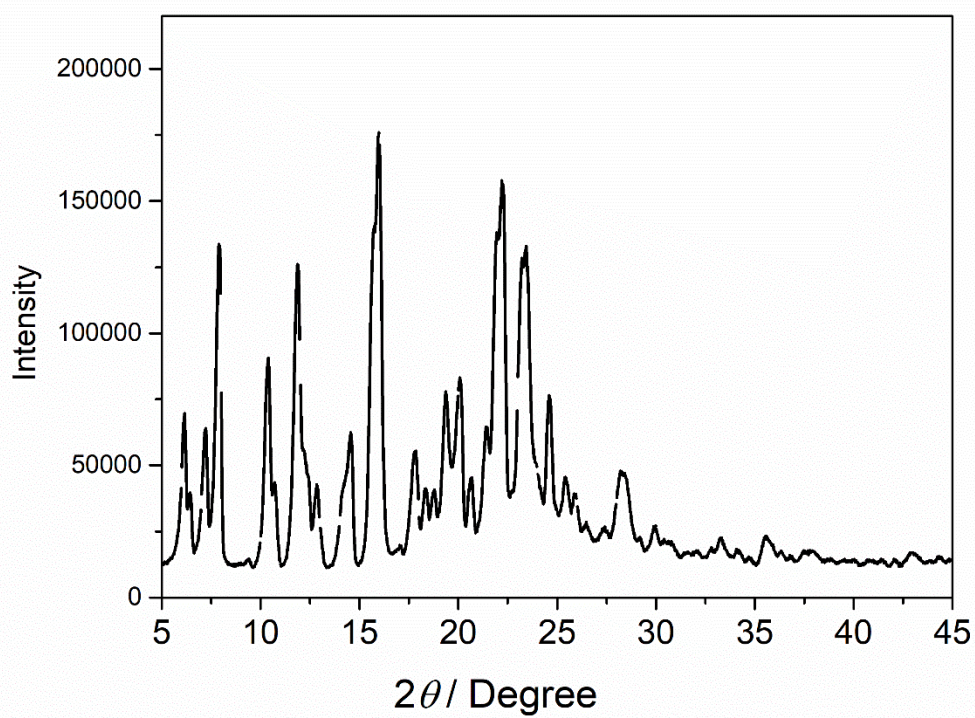


Fig. S5. PXRD pattern of **EtP5 α**

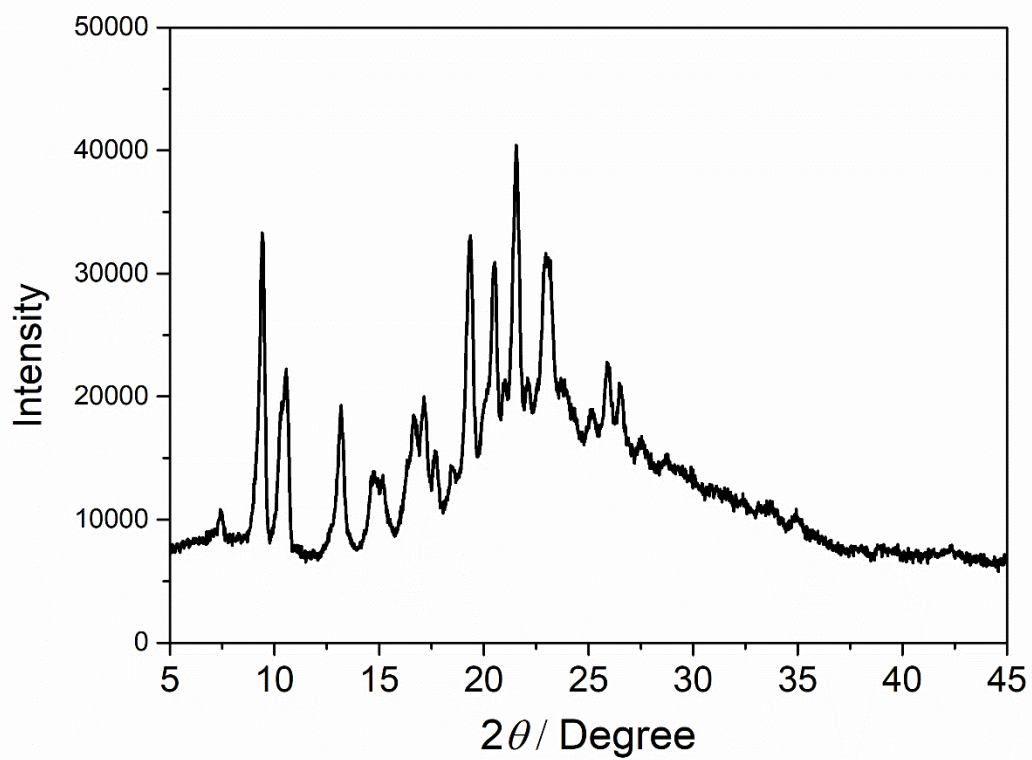


Fig. S6. PXRD pattern of **EtP6 β** .

5. Vapor-Phase Adsorption Measurements

5.1. Single-Component THF and pyrrolidine adsorption

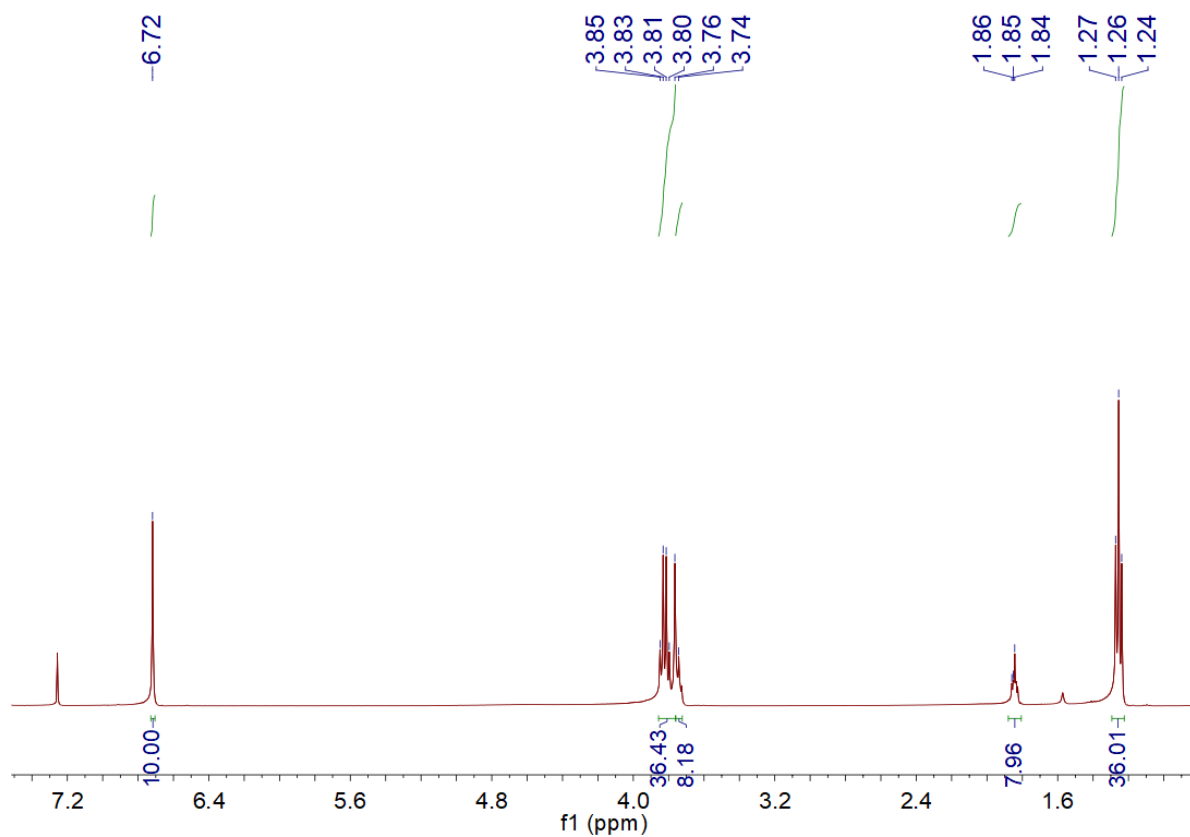


Fig. S7. ^1H NMR spectrum (400 MHz, CDCl_3 , 298 K) of **EtP5** α after adsorption of THF vapor.

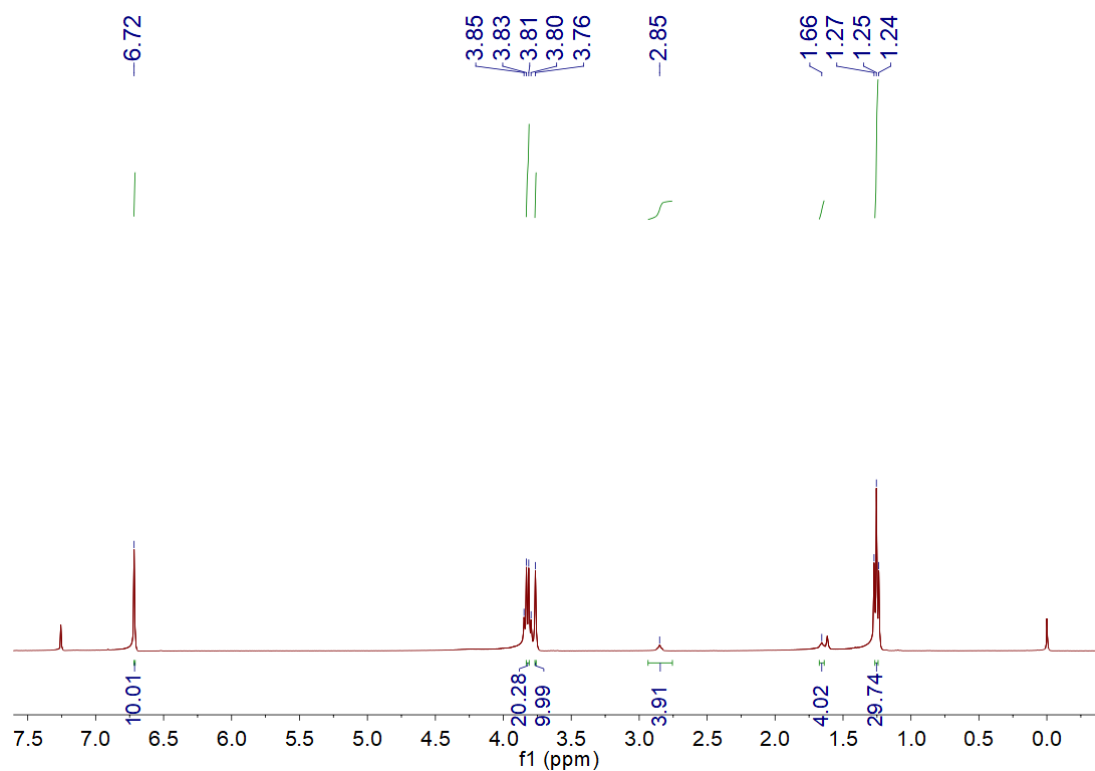


Fig. S8. ^1H NMR spectrum (400 MHz, CDCl_3 , 298 K) of **EtP5** α after adsorption of pyrrolidine vapor.

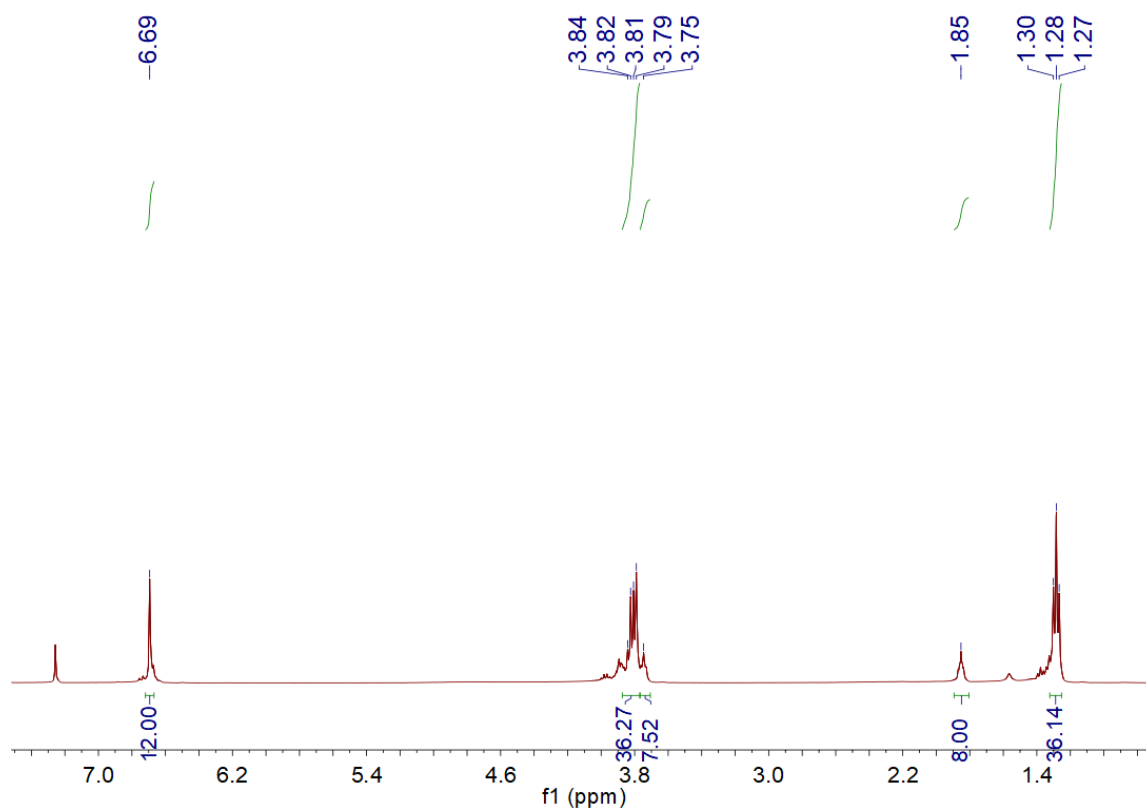


Fig. S9. ^1H NMR spectrum (400 MHz, CDCl_3 , 298 K) of **EtP6 β** after adsorption of THF vapor.

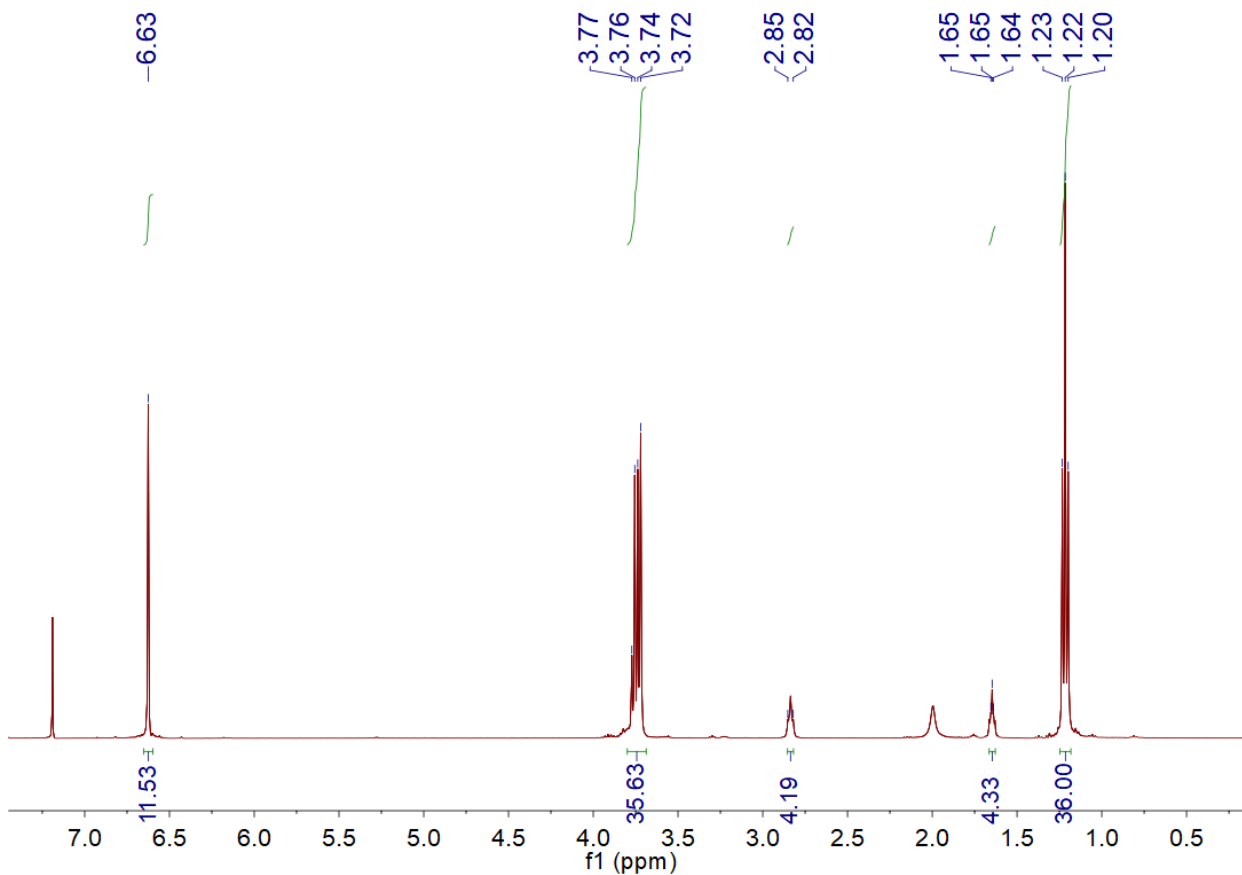


Fig. S10. ^1H NMR spectrum (400 MHz, CDCl_3 , 298 K) of **EtP6 β** after adsorption of pyrrolidine vapor.

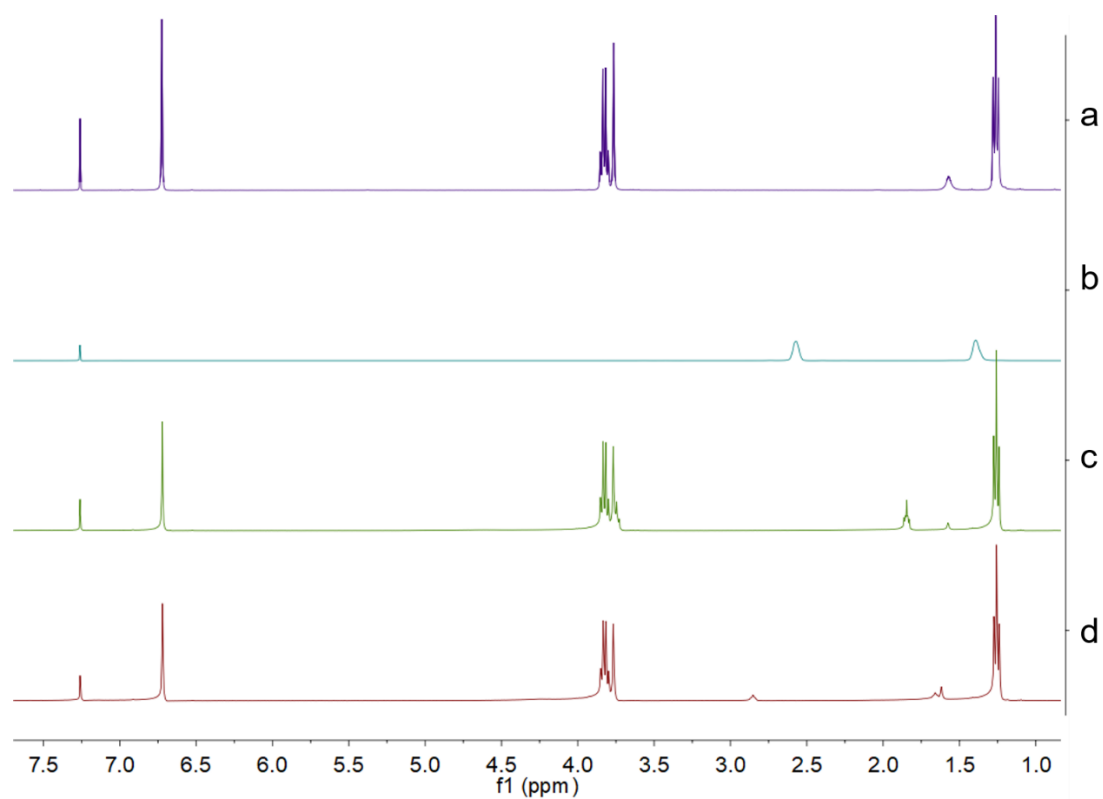


Fig. S11. ¹H NMR spectra (400 MHz, CDCl₃, 298 K): (a) **EtP5**; (b) pyrrolidine; (c) a mixture of THF and **EtP5**; (d) a mixture of pyrrolidine and **EtP5**.

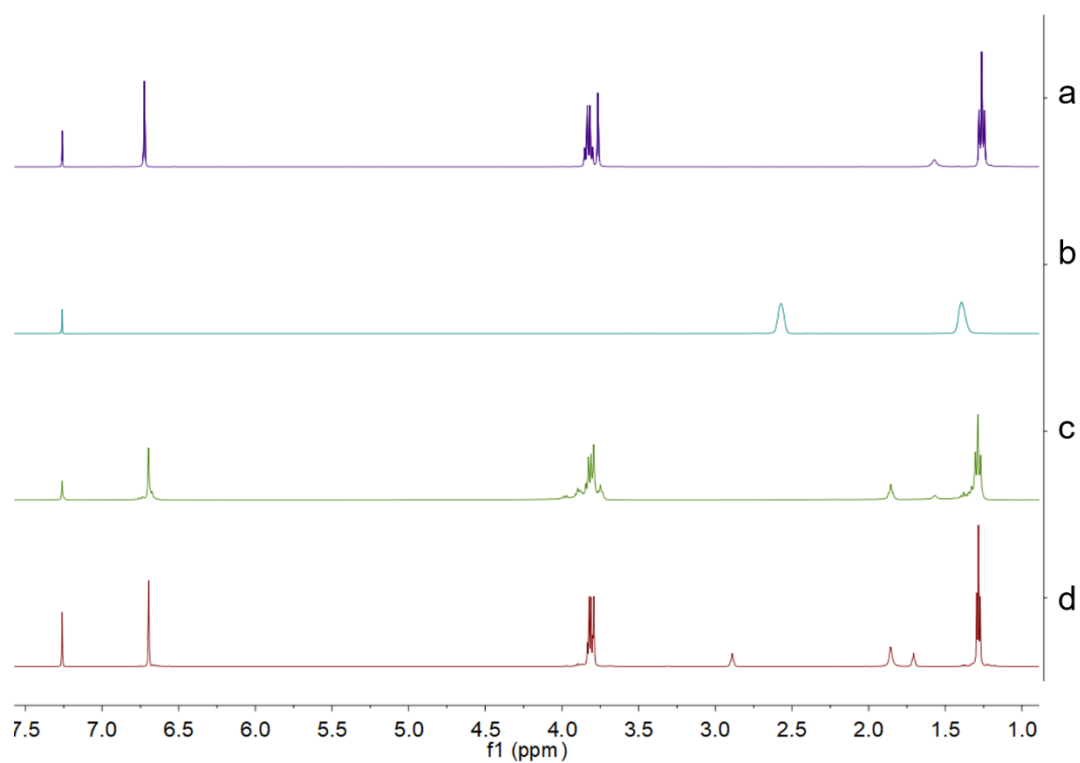


Fig. S12. ¹H NMR spectra (400 MHz, CDCl₃, 298 K): (a) **EtP6**; (b) pyrrolidine; (c) a mixture of THF and **EtP6**; (d) a mixture of pyrrolidine and **EtP6**.

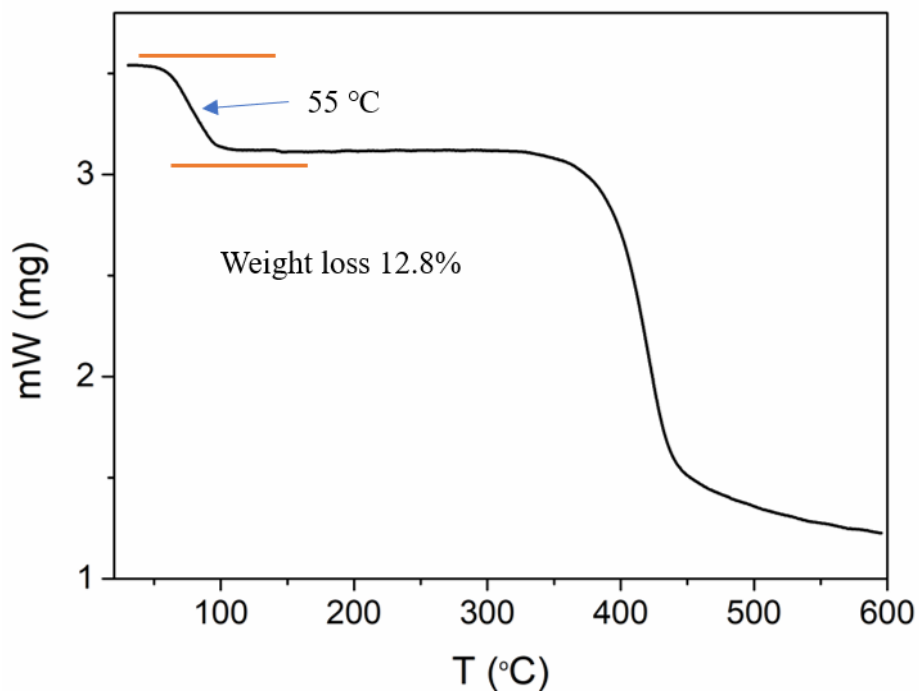


Fig. S13. TGA curve of desolvated **EtP5 α** after sorption of THF vapor. The weight loss below 100 °C can be calculated as two THF molecules per **EtP5** molecule.

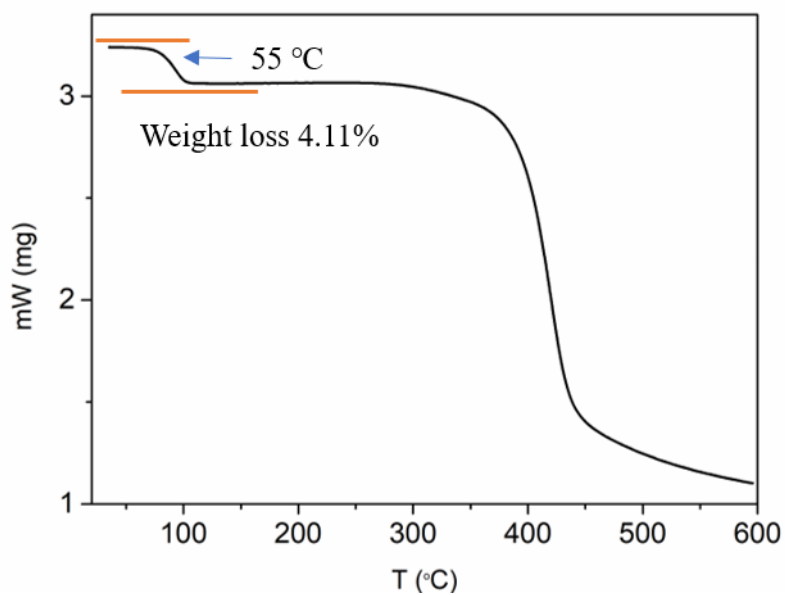


Fig. S14. TGA curve of desolvated **EtP5 α** after sorption of pyrrolidine vapor. The weight loss below 120 °C can be calculated as one pyrrolidine molecule per **EtP5** molecule.

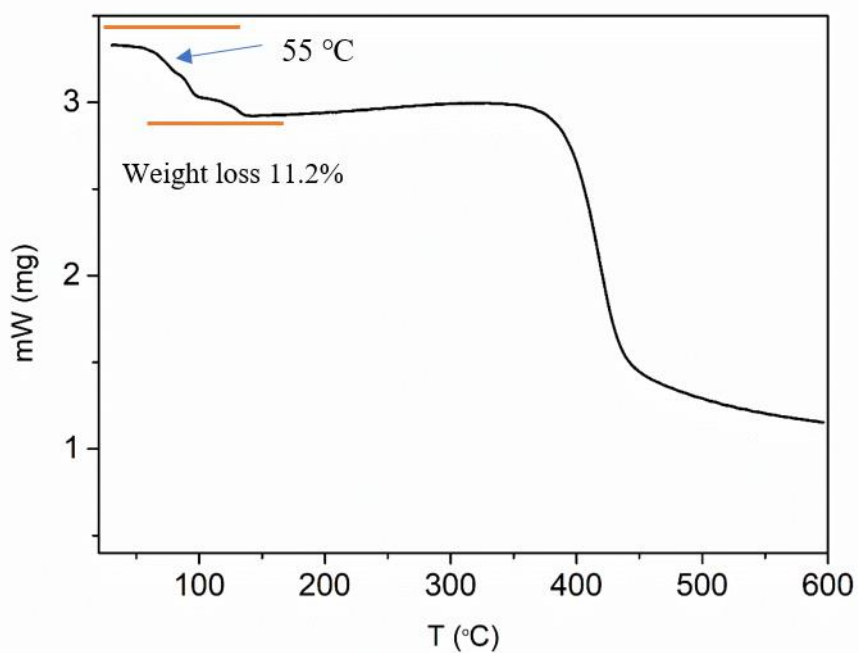


Fig. S15. TGA of desolvated **EtP6 β** after sorption of THF vapor. The weight loss below 150 °C can be calculated as two THF molecule per **EtP6** molecule.

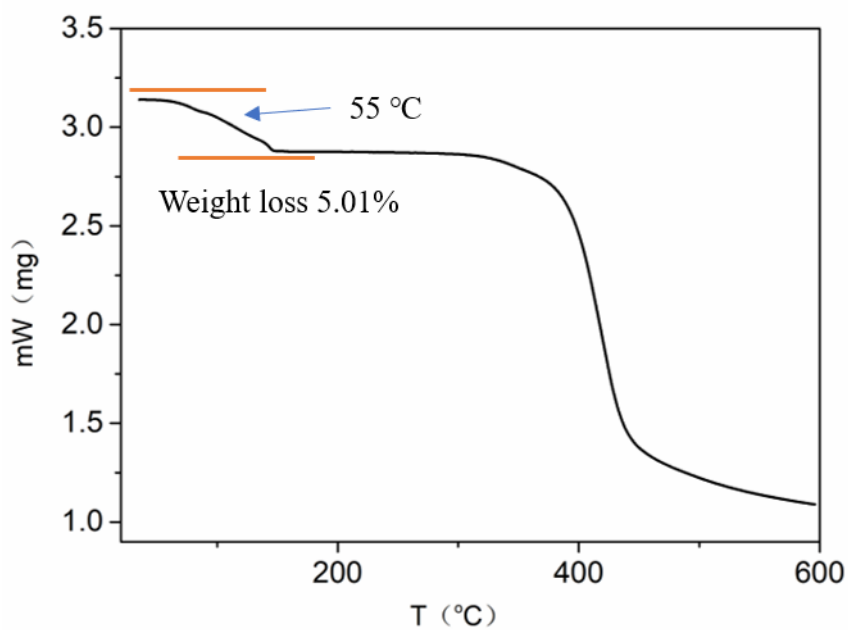


Fig. S16. TGA curve of desolvated **EtP6 β** after sorption of pyrrolidine vapor. The weight loss below 150 °C can be calculated as one pyrrolidine molecule per **EtP6** molecule.

5.2. Structural analyses after single-component vapor adsorption

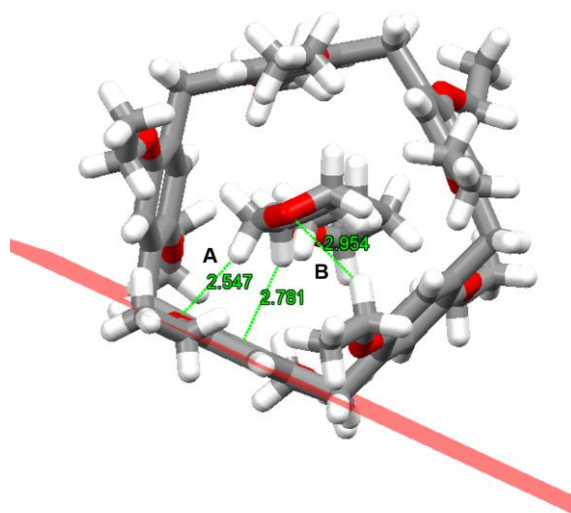


Fig. S17. Single crystal structure of 2THF@EtP5. C-H...O distances (Å) and C-H...O angles (deg) of hydrogen bonds: (A) 2.547, 111.82; (B) 2.954, 141.57. C-H... π distance (Å): 2.781.

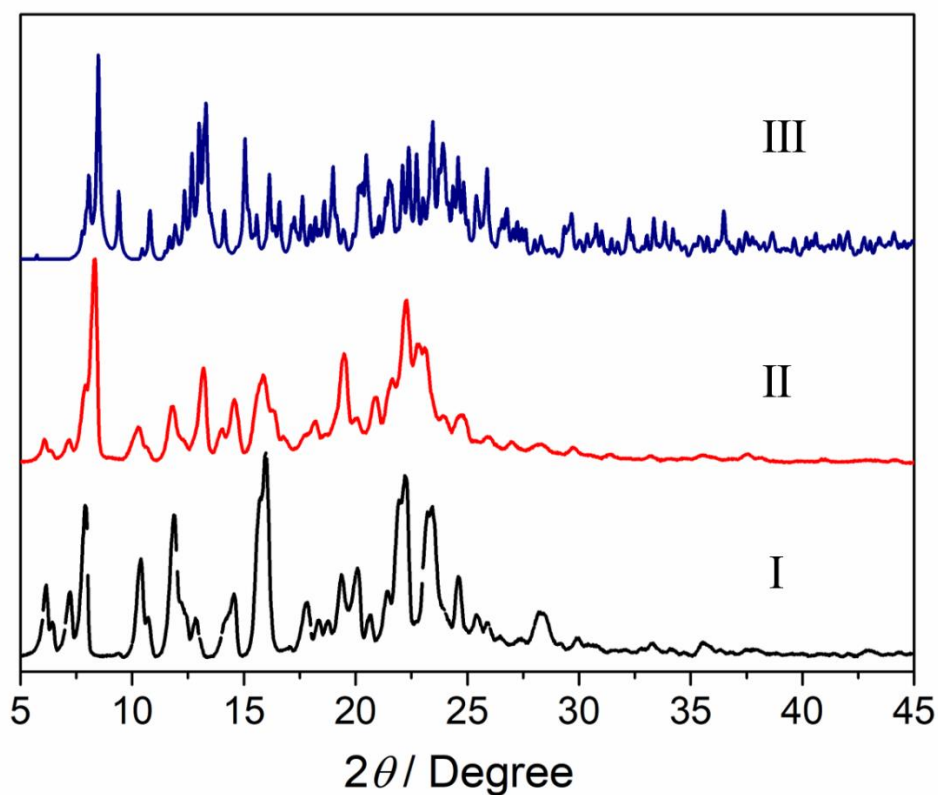


Fig. S18. PXRD of EtP5: (I) original EtP5 α ; (II) after adsorption of THF vapor; (III) simulated from the single crystal structure of 4THF@2EtP5.

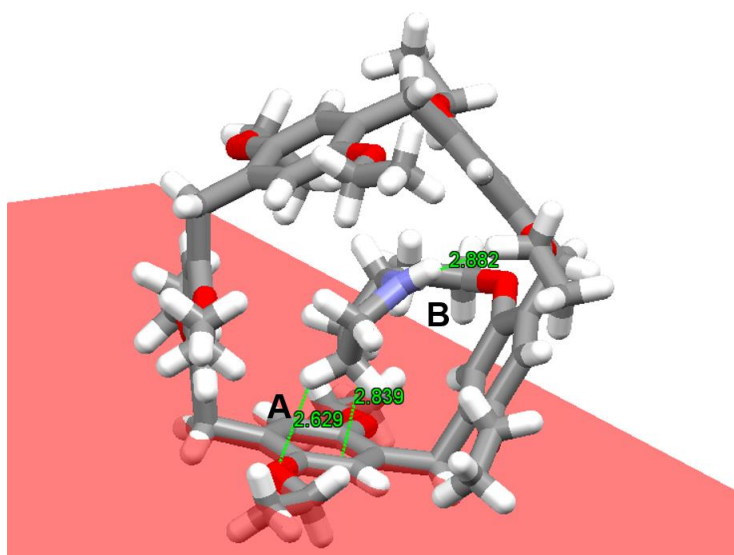


Fig. S19. Single crystal structure of pyrrolidine@EtP5. C–H···O distance (Å) and C–H···O angle (deg) of hydrogen bond **A**: 2.629, 101.20; N–H···O distance (Å) and N–H···O angle (deg) of hydrogen bond **B**: 2.882, 119.41; C–H··· π distance (Å): 2.839.

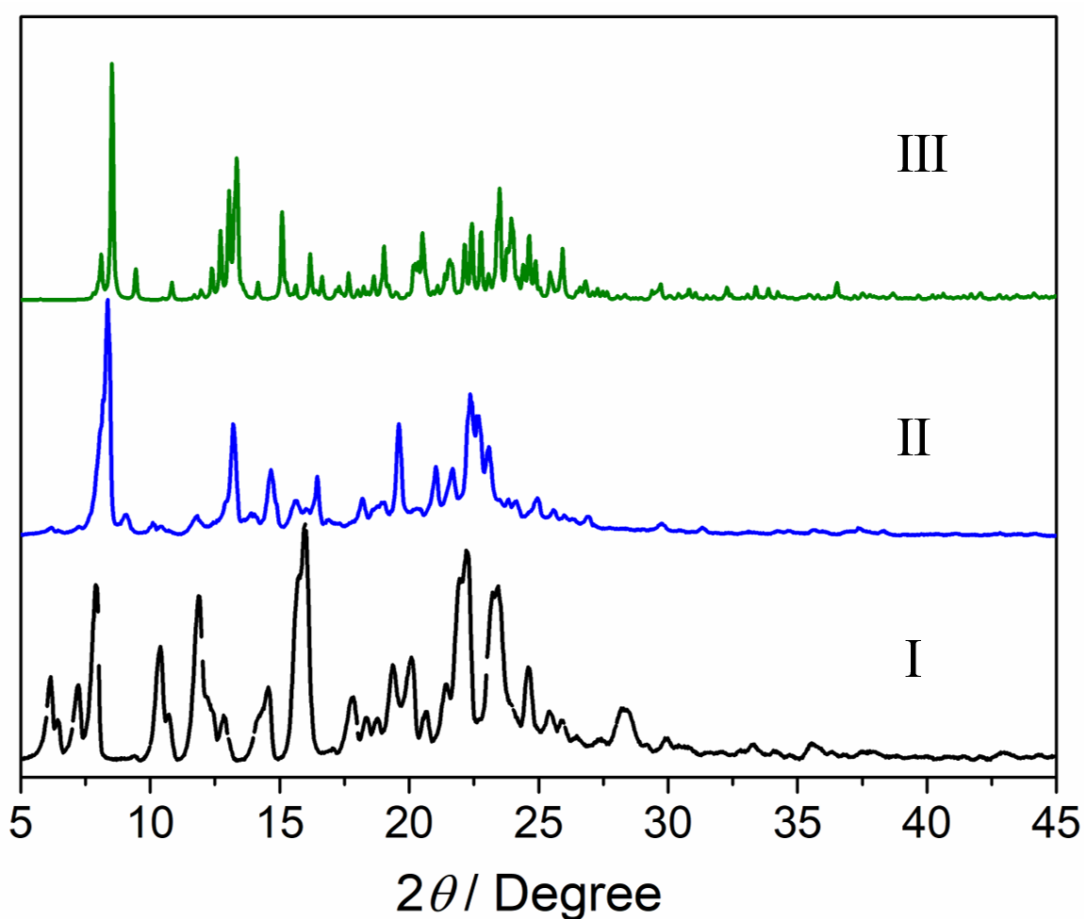


Fig. S20. PXRD of EtP5: (I) original EtP5 α ; (II) after adsorption of pyrrolidine vapor; (III) simulated from the single crystal structure of pyrrolidine@EtP5.

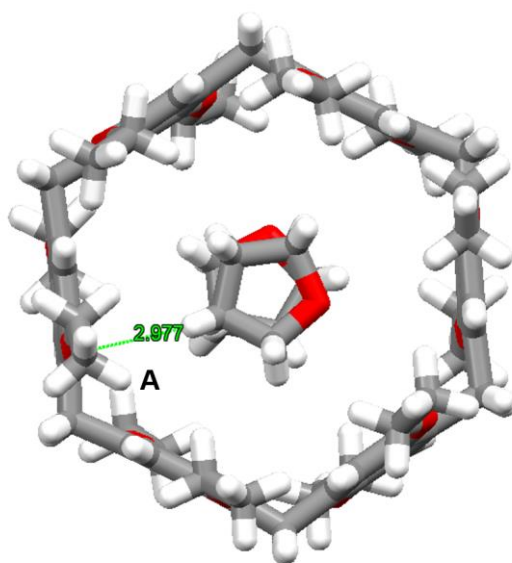


Fig. S21. Single crystal structure of 2THF@EtP6. C-H \cdots O distance (Å) and C-H \cdots O angle (deg) of hydrogen bond A: 2.977, 101.93.

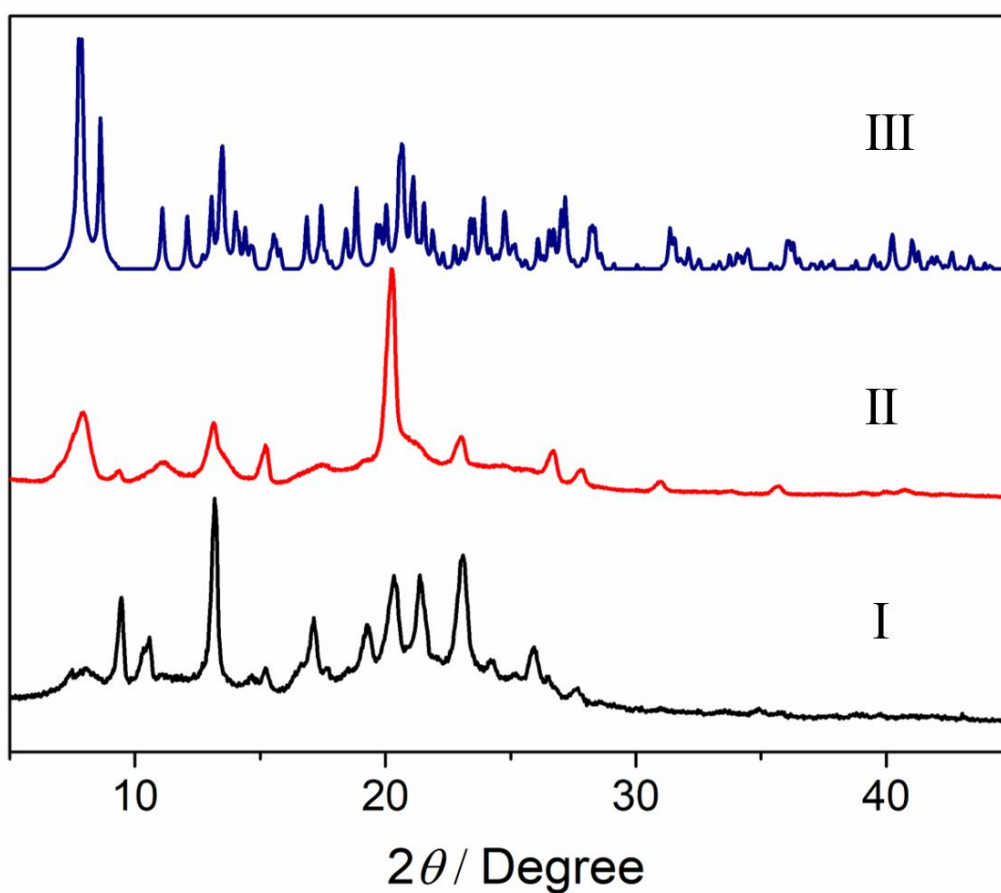


Fig. S22. PXRD patterns of EtP5: (I) original EtP6 β ; (II) after adsorption of THF vapor; (III) simulated from the single crystal structure of 2THF@EtP6.

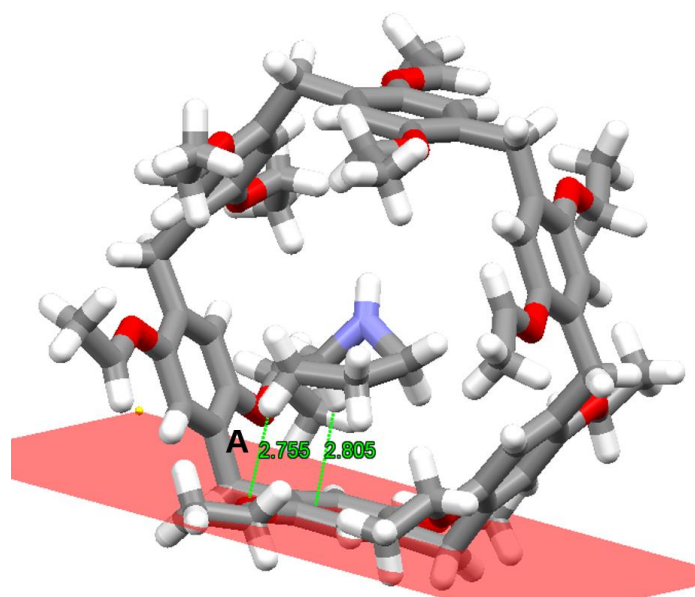


Fig. S23. Single crystal structure of pyrrolidine@EtP6. C–H···O distance (Å) and C–H···O angle (deg) of the hydrogen bond: 2.755, 143.99; C–H··· π distance (Å): 2.805.

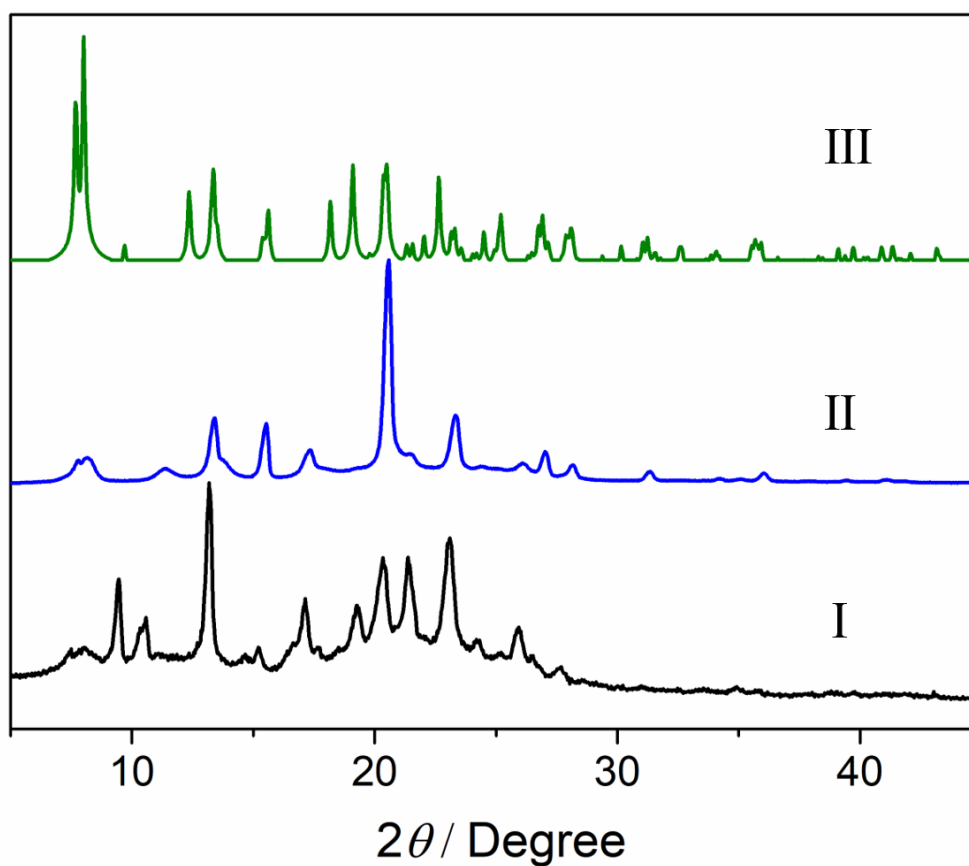


Fig. S24. PXRD patterns of EtP6: (I) original EtP6 β ; (II) after adsorption of pyrrolidine vapor; (III) simulated from the single crystal structure of pyrrolidine@EtP6.

5.3. Uptakes of THF and pyrrolidine in **EtP5 α**

For each experiment, an open 5.00 mL vial containing 20.00 mg of guest-free **EtP5 α** adsorbent was placed in a sealed 20.00 mL vial containing 1.00 mL of a 50:50 v/v THF and pyrrolidine mixture. The relative uptake of THF or pyrrolidine by **EtP5 α** was measured by heating the crystals to release the adsorbed vapor using GC. Before measurements, the crystals were placed in the air for 12 h to remove the surface-physically adsorbed vapor.

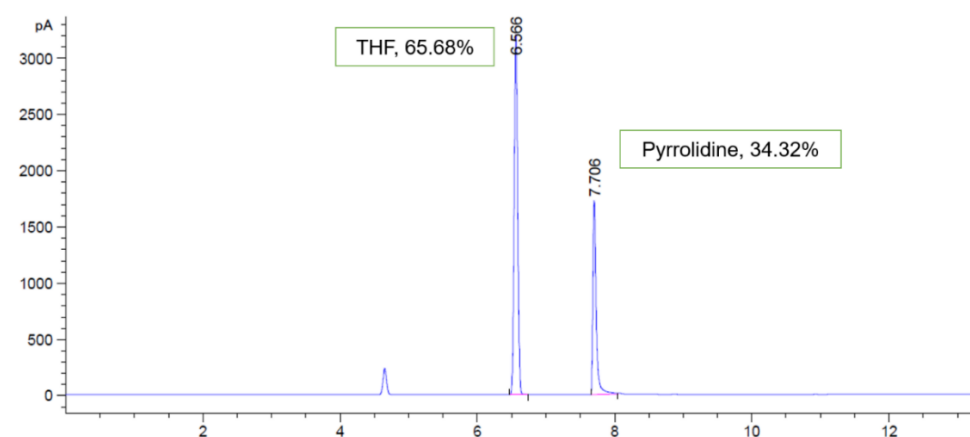


Fig. S25. Relative uptake of the THF/Pyrrolidine mixture (v:v = 50:50) adsorbed in **EtP5 α** after 6 hours using gas chromatography.

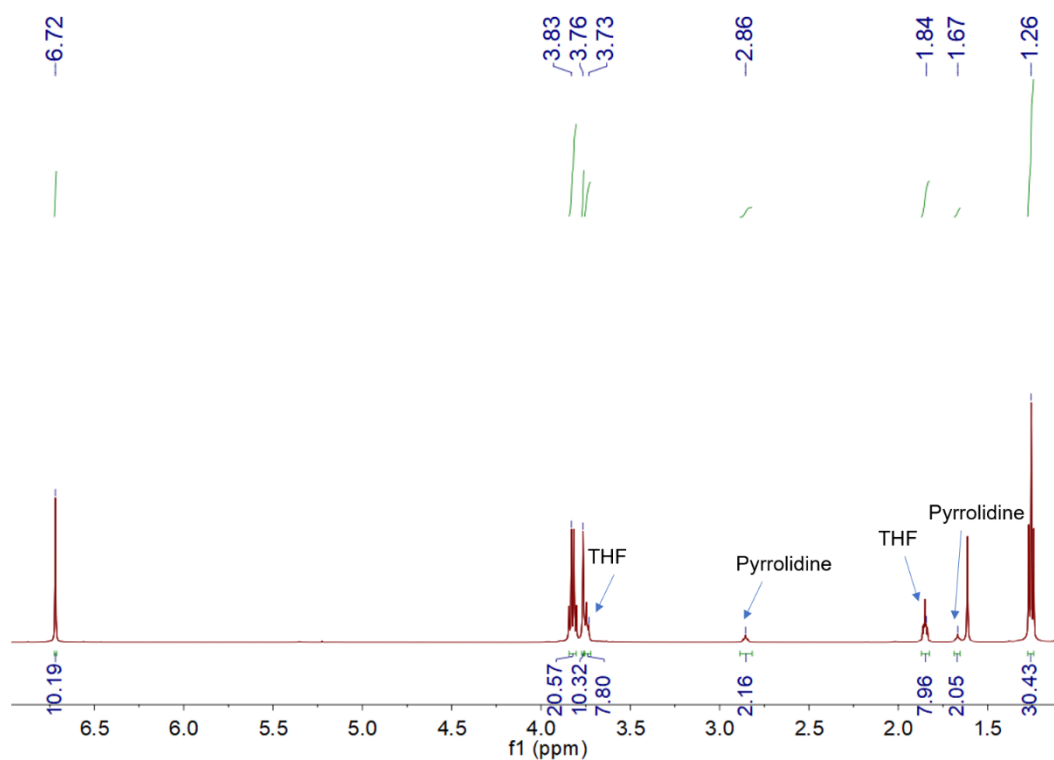


Fig. S26. ¹H NMR spectrum (600 MHz, CDCl₃, 298 K) of **EtP5 α** after adsorption of the THF and pyrrolidine mixture vapor (v:v = 50:50).

5.4. Uptakes of THF and pyrrolidine in **EtP6 β**

For each experiment, an open 5.00 mL vial containing 20.00 mg of guest-free **EtP6 β** adsorbent was placed in a sealed 20.00 mL vial containing 1.00 mL of 50:50 v/v THF and pyrrolidine mixture. The relative uptake of THF or pyrrolidine by **EtP6 β** was measured by heating the crystals to release the adsorbed vapor using gas chromatography. Before measurements, the crystals were placed for 12 h in the air to remove the surface-physically adsorbed vapor.

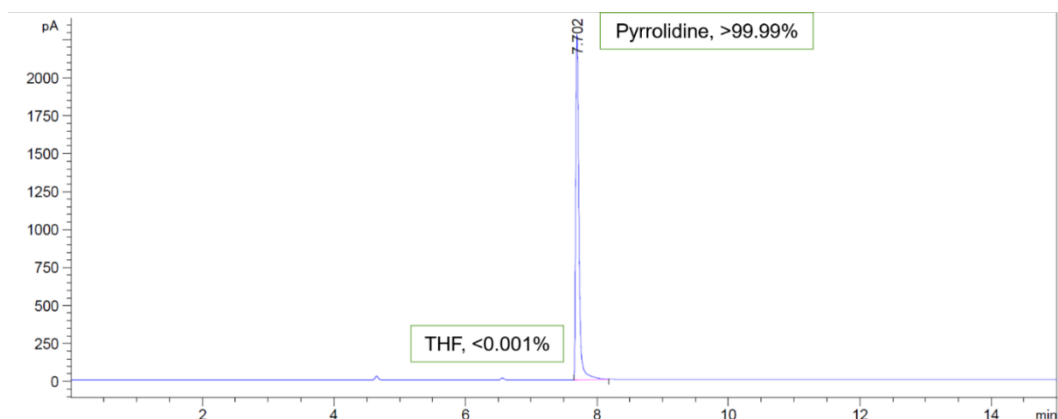


Fig. S27. Relative uptake of the THF/pyrrolidine mixture (v:v = 50:50) adsorbed in **EtP6 β** after 2 hours using GC.

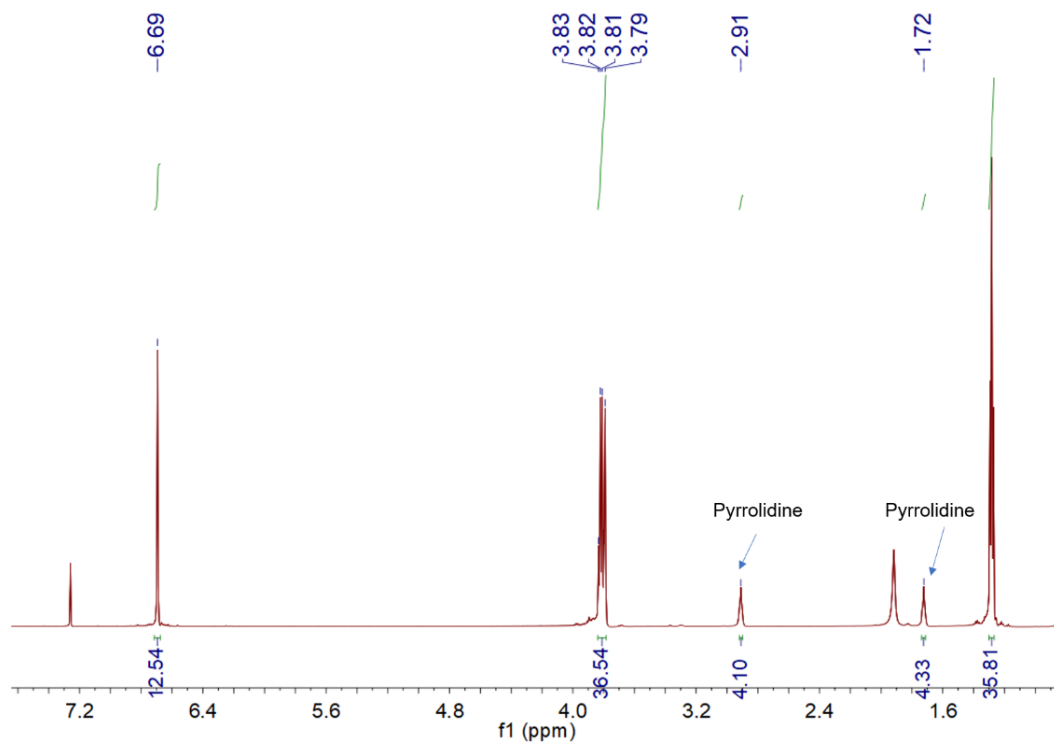


Fig. S28. ^1H NMR spectrum (600 MHz, CDCl_3 , 298 K) of **EtP6 β** after adsorption of the THF and pyrrolidine mixture vapor (v:v = 50:50).

6. Recyclability of **EtP6** β

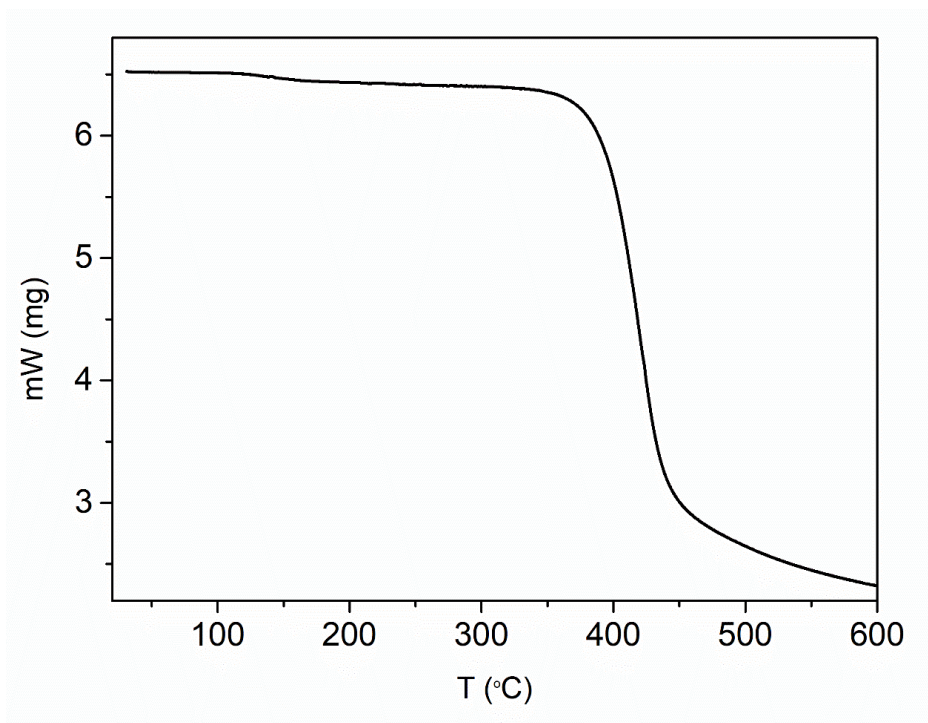


Fig. S29. TGA curve of desolvated pyrrolidine@**EtP6** upon removal of pyrrolidine.

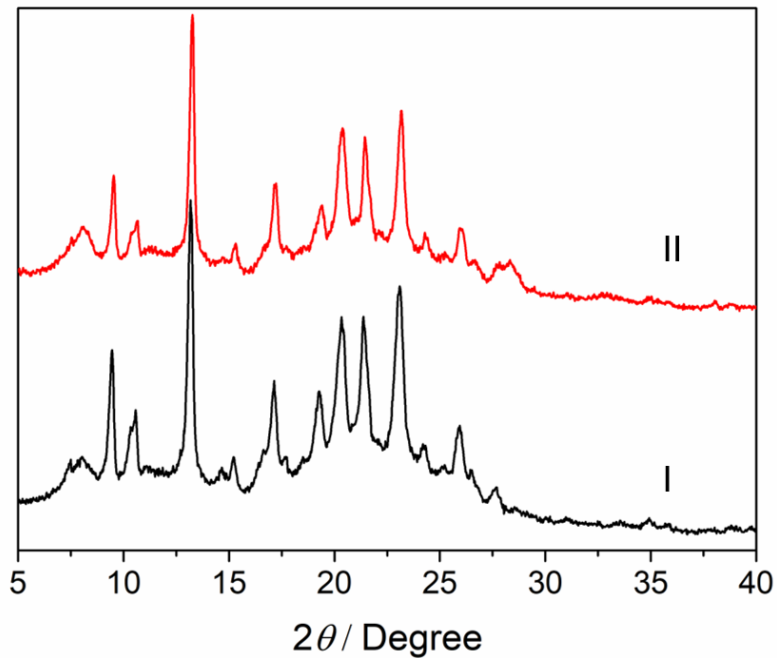


Fig. S30. PXRD of **EtP6**: (I) original **EtP6** β ; (II) desolvated pyrrolidine@**EtP6**. This means that upon removal of pyrrolidine, pyrrolidine@**EtP6** transforms back to **EtP6** β .

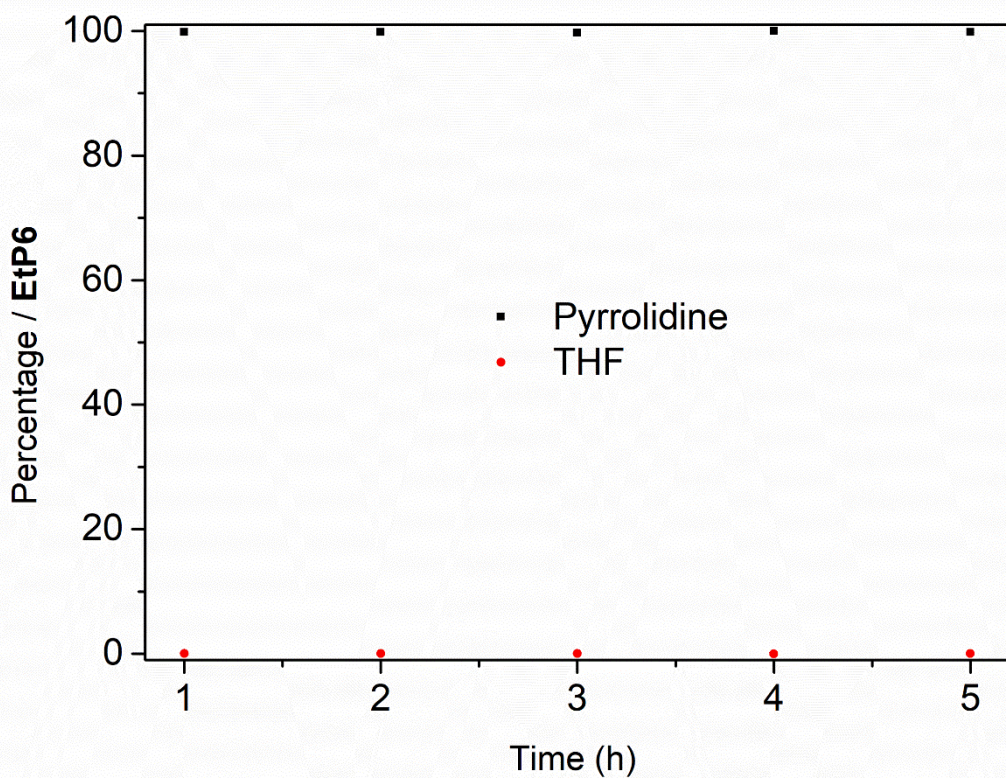


Fig. S31. Relative uptakes of THF and pyrrolidine by **EtP6 β** over 2 h after **EtP6 β** was recycled five times.

7. References

- S1 Hu, X.-B.; Chen, Z.; Zhang, L.; Hou, J.-L.; Li, Z.-T. *Chem. Commun.* 2012, **48**, 10999.
- S2 Jie, K.; Liu, M.; Zhou, Y.; Little, M. A.; Pulido, A.; Chong, S. Y.; Stephenson, A.; Hughes, A. R.; Sakakibara, F.; Ogoshi, T.; Blanc, F.; Day, G. M.; Huang, F.; A. I. Cooper. *J. Am. Chem. Soc.* 2018, **140**, 6921.